Experimental and theoretical investigations of an air-slot coupler between dielectric and plasmonic waveguides

Rami A. Wahsheh[1,*] and Mustafa A. G. Abushagur[2]

[1]*Communications Engineering Department, King Abdullah II Faculty of Engineering, Princess Sumaya University for Technology, Al-Jubaiha, Amman 11941, Jordan*
[2]*Microsystems Engineering, Kate Gleason College of Engineering, Rochester Institute of Technology, Rochester, New York 14623, USA*
[*]*r.wahsheh@psut.edu.jo*

Abstract: In this paper, we experimentally show an effective method of coupling light between dielectric waveguides and metal-dielectric-metal plasmonic waveguides using an air-slot waveguide that extends into both types of waveguides. Our experimental results validate the theoretical calculation results of the proposed coupler. In addition, we investigated the sensitivity of our design to different fabrication challenges that may result in changing the width and length of the targeted optimum values in our design. Numerical simulation results show that the cut-off wavelength can be shifted by either changing the width of the dielectric or slot waveguide. The shift occurs because, as the waveguide's width changes, the mode size changes and consequently the impedance mismatch between the dielectric and slot waveguide changes. We also found that changing the position of the air-slot waveguide with respect to the center of the dielectric waveguide resulted in a reduction in the coupling efficiency due to the reduction in the overlapped area between the mode supported by the slot waveguide and that of the dielectric waveguide.

OCIS codes: (130.3120) Integrated optics devices; (230.7370) Waveguides; (240.6680) Surface plasmons.

References and links

1. R. A. Wahsheh, Z. Lu, and M. A. G. Abushagur, "Integrated Nanoplasmonic Splitter," *International Symposium on High Capacity Optical Networks and Enabling Technologies* (HONET, 2013), pp. 155–156.
2. R. A. Wahsheh, Z. Lu, and M. A. G. Abushagur, "Nanoplasmonic Directional Couplers and Mach-Zehnder Interferometers," Opt. Commun. **282**(23), 4622–4626 (2009).
3. B. Wang and G. P. Wang, "Plasmon Bragg Reflectors and Nanocavities on Flat Metallic Surfaces," Appl. Phys. Lett. **87**(1), 013107 (2005).
4. H. Lu, X. Liu, Y. Gong, D. Mao, and L. Wang, "Enhancement of Transmission Efficiency of Nanoplasmonic Wavelength Demultiplexer Based on Channel Drop Filters and Reflection Nanocavities," Opt. Express **19**(14), 12885–12890 (2011).
5. K. Wen, L. Yan, W. Pan, B. Luo, Z. Guo, and Y. Guo, "A Four-Port Plasmonic Quasi-Circulator Based on Metal-Insulator-Metal Waveguides," Opt. Express **20**(27), 28025–28032 (2012).
6. Y. Gong, X. Liu, and L. Wang, "High-Channel-Count Plasmonic Filter with the Metal-Insulator-Metal Fibonacci-Sequence Gratings," Opt. Lett. **35**(3), 285–287 (2010).
7. G. Wang, H. Lu, X. Liu, and Y. Gong, "Numerical Investigation of an All-Optical Switch in a Graded Nonlinear Plasmonic Grating," Nanotechnology **23**(44), 444009 (2012).
8. E. N. Economou, "Surface Plasmons in Thin Films," Phys. Rev. **182**(2), 539–554 (1969).
9. S. A. Maier, P. G. Kik, H. A. Atwater, S. Meltzer, E. Harel, B. E. Koel, and A. A. Requicha, "Local Detection of Electromagnetic Energy Transport Below the Diffraction Limit In Metal Nanoparticle Plasmon Waveguides," Nat. Mater. **2**(4), 229–232 (2003).
10. K. H. Wen, L. S. Yan, W. Pan, B. Luo, Z. Guo, Y. H. Guo, and X. G. Luo, "Spectral Characteristics of Plasmonic Metalinsulator-Metal Waveguides with a Tilted Groove," IEEE Photonics J. **4**(5), 1794–1800 (2012).
11. F. Hu, H. Yi, and Z. Zhou, "Wavelength Demultiplexing Structure Based on Arrayed Plasmonic Slot Cavities," Opt. Lett. **36**(8), 1500–1502 (2011).
12. Y.-J. Hsu and Y. Lai, "Vertical Plasmonic Resonance Coupler," Opt. Express **23**(1), 292–300 (2015).

#254165 Received 23 Nov 2015; revised 16 Feb 2016; accepted 19 Feb 2016; published 7 Apr 2016

13. X. Han, "Dual-Channel Dispersionless Slow Light Based on Plasmon-Induced Transparency," Appl. Opt. **53**(1), 9–13 (2014).
14. G. Veronis and S. Fan, "Theoretical Investigation of Compact Couplers Between Dielectric Slab Waveguides and Two-Dimensional Metal-Dielectric-Metal Plasmonic Waveguides," Opt. Express **15**(3), 1211–1221 (2007).
15. C.-T. Chen, X. Xu, A. Hosseini, Z. Pan, H. Subbaraman, X. Zhang, and R. T. Chen, "Design of Highly Efficient Hybrid Si-Au Taper for Dielectric Strip Waveguide to Plasmonic Slot Waveguide Mode Converter," J. Lightwave Technol. **33**(2), 535–540 (2015).
16. Z. Han, A. Y. Elezzabi, and V. Van, "Experimental Realization of Subwavelength Plasmonic Slot Waveguides on a Silicon Platform," Opt. Lett. **35**(4), 502–504 (2010).
17. R. A. Wahsheh, Z. Lu, and M. A. G. Abushagur, "Nanoplasmonic Couplers and Splitters," Opt. Express **17**(21), 19033–19040 (2009).
18. R. A. Wahsheh, Z. Lu, and M. Abushagur, "Experimental Investigation of a Nanoplasmonic Air-Slot Coupler Toward Dense Optical Integrated Circuits," in *Frontiers in Optics 2015*, OSA Technical Digest (Optical Society of America, 2015), paper FW3E.2.
19. R. Yang, R. A. Wahsheh, Z. Lu, and M. A. G. Abushagur, "Efficient Light Coupling Between Dielectric Slot Waveguide and Plasmonic Slot Waveguide," Opt. Lett. **35**(5), 649–651 (2010).
20. D. Kong and M. Tsubokawa, "Evaluation of Slot-To-Slot Coupling Between Dielectric Slot Waveguides and Metal-Insulator-Metal Slot Waveguides," Opt. Express **23**(15), 19082–19091 (2015).

1. Introduction

Hybrid integration of dielectric and plasmonic waveguides is necessary to reduce the propagation losses due to metallic interaction. Accordingly, the dielectric waveguide is used to couple light into and out of the plasmonic waveguides. In order to support nanofabrication of plasmonic devices such as splitters [1], Mach-Zehnder interferometers [2], reflectors [3], wavelength demultiplexers [4], circulators [5], filters [6], and all-optical switching [7], the interface between the dielectric and plasmonic waveguides should be designed carefully to minimize back reflection and increase the coupling efficiency. Many plasmonic guiding structures have been proposed such as metal-insulator-metal (MIM) waveguides [8], metal nanoparticle plasmon waveguides [9], metallic grooves waveguides [10], plasmonic slot cavities [11], and plasmonic grating couplers [12]. The most promising type of waveguide is the MIM waveguide which attracted a lot of attention because it is easy to fabricate without the need of high precision fabrication techniques, in addition to its ability to tightly confine light in nanometer wide slots which makes it possible to tailor its optical properties [13].

Several structures have been reported and investigated to increase the coupling efficiency from a dielectric waveguide into a MIM plasmonic waveguide [14–18]. One solution in the literature proposes using a multi-section taper inside both the dielectric and plasmonic waveguides [14]. The proposed structure is not practical to fabricate and a special software is needed to design the multi-section taper. Another solution in the literature proposes using adiabatic mode conversion by tapering both the dielectric and plasmonic waveguides [15,16]. The length of the taper is too long for ultracompact integrated circuits. Another solution in the literature that has attracted a lot of attention proposes using a very compact coupler at the interface between the plasmonic and dielectric waveguides [17]. The proposed coupler provided a large fabrication tolerance if the coupler is fabricated inside the plasmonic waveguide at the interface with the dielectric waveguide. It is almost impossible to fabricate the coupler that exactly starts at the interface with the dielectric waveguide without leaving either a gap between them or having the coupler on top of the dielectric waveguide. In either case, back reflection will be high. In [18], we proposed an air-slot waveguide that is located inside both the dielectric and plasmonic waveguides. The proposed coupler can be fabricated in which light couples from the dielectric waveguide into the dielectric air-slot waveguide before it is coupled into the plasmonic waveguide. The slot-waveguide is inside both types of waveguides because it is impossible to fabricate the plasmonic slot-waveguide that is sandwiched between the two dielectric waveguides without creating an air slot-waveguide inside the dielectric waveguide. The air-slot waveguide inside the dielectric waveguide ensures that light couples from the dielectric waveguide into and out of the plasmonic waveguide. In this paper, we show the design, fabrication steps, and experimental results of an air-slot coupler between a silicon waveguide and a gold-air-gold plasmonic waveguide. We also show the sensitivity of our design to different fabrication challenges.

#254165 Received 23 Nov 2015; revised 16 Feb 2016; accepted 19 Feb 2016; published 7 Apr 2016

The two-dimensional (2D) finite-difference time-domain method is used in the design and analysis of the proposed air-slot coupler. A three-dimensional (3D) simulation was not used because the run time and memory requirements for a 3D simulation is far much more than that for a 2D simulation. In the future, we plan to use a 3D simulation using software including MIT electromagnetic equation propagation (MEEP). We used a uniform mesh size of 1 nm to accurately capture the changes of the field at the interface of both of the dielectric and plasmonic air-slot waveguides. The dielectric material is silicon and the metal material is gold. The dielectric constant of silicon and gold at 1550 nm are 12.11 and –92.946 + i11.096, respectively. The coupling efficiency in our analysis is calculated by normalizing the output power measured at the second (output) dielectric waveguide with respect to the input power of the launched light.

2. Air-slot coupler design and fabrication

We fabricated the plasmonic air-slot coupler that is shown in Fig. 1(a) on a silicon-on-insulator wafer. Scanning electron microscope image of the fabricated device is shown in Fig. 1(b). The height of the silicon and plasmonic waveguides is 250 nm. Three e-beam lithographies were used: one to define the alignment marks, another one to place the dielectric waveguides at specific locations from the alignment marks, and the last one to define the areas where gold is deposited. We then used the focused ion beam (FIB) to define the slot waveguides. We deposited a platinum layer on top of the gold layer using the FIB tool before defining the slot waveguides. This was done to get vertical sidewalls of the slot waveguides instead of slightly angled ones. Part of the silicon waveguide at each end of the plasmonic air-slot waveguide was milled [denoted by L_c in Fig. 1(a)] to make sure that light couples from the dielectric waveguide into the plasmonic air-slot waveguide.

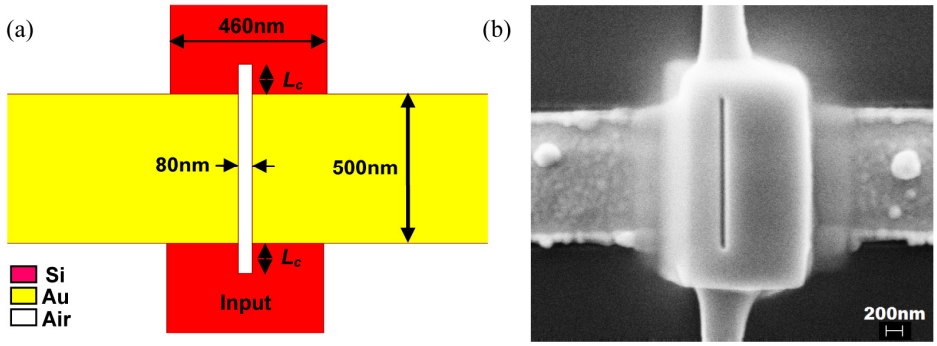

Fig. 1. (a) Schematic of the plasmonic air-slot coupler. (b) Scanning electron microscope image of the fabricated air-slot coupler.

Having the dielectric air-slot waveguide at the interface with the plasmonic waveguide is expected to increase the coupling efficiency because the field inside the dielectric air-slot waveguide matches that in the plasmonic air-slot waveguide [19,20]. To show this numerically, we varied L_c in both dielectric waveguides at the same time and measured the corresponding coupling efficiency at the output dielectric waveguide (see Fig. 2). We found that the coupling efficiency of the coupler at 1550 nm increased by about 20% when L_c = 50 nm. The oscillation in the measured coupling efficiency is due to the Fabry-Perot cavity response that is caused by the reflection of the mode from each dielectric waveguide.

#254165 Received 23 Nov 2015; revised 16 Feb 2016; accepted 19 Feb 2016; published 7 Apr 2016

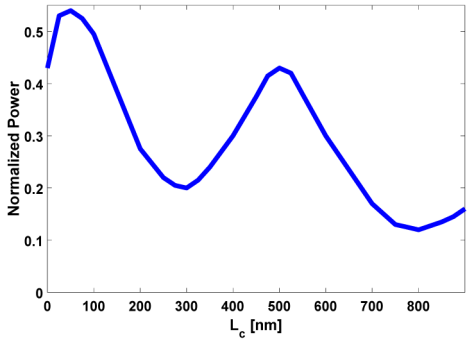

Fig. 2. Coupling efficiency as a function of the silicon air-slot waveguide's length, L_c.

3. Experimental results

We tested the plasmonic air-slot coupler that is shown in Fig. 1(b). The output light power was measured as the wavelength of a tunable laser source was scanned from 1260 to 1620 nm. A polarization controller was used to allow TM-like modes to couple into the silicon waveguide. Coupling into and out of the silicon waveguides was achieved using tapered micro-lens fibers with a spot diameter of 2.5 ± 0.5 micron. Translational stages were used to align the input and output fibers to the device being tested. The output power was measured using an infrared detector and recorded using a power meter. As shown in Fig. 3(a), the measured spectrum of the fabricated plasmonic coupler has a trend similar to that of simulation, except that it is shifted by 110 nm. All the theoretical and experimental results in Fig. 3(a) were normalized with respect to the maximum theoretical calculated power (i.e., 72% at a wavelength of 1620 nm). This is done to show the percentage of the measured power at each wavelength with respect to that of simulation. The 110 nm shift was expected because of the sensitivity of the device to different lithography and etching bias. The fabrication limitations resulted in fabricating waveguides of widths different than the targeted values. The targeted width of the silicon and air-slot waveguides were 460 nm and 80 nm, respectively while the measured value for the former one was 500 nm and that for the latter one was 75 nm. This caused the cut-off wavelength to shift to the right (i.e., at a higher wavelength) and caused the coupling efficiency to decrease [see Fig. 3(b)]. The lithography and etching bias is discussed in more depth in the next section.

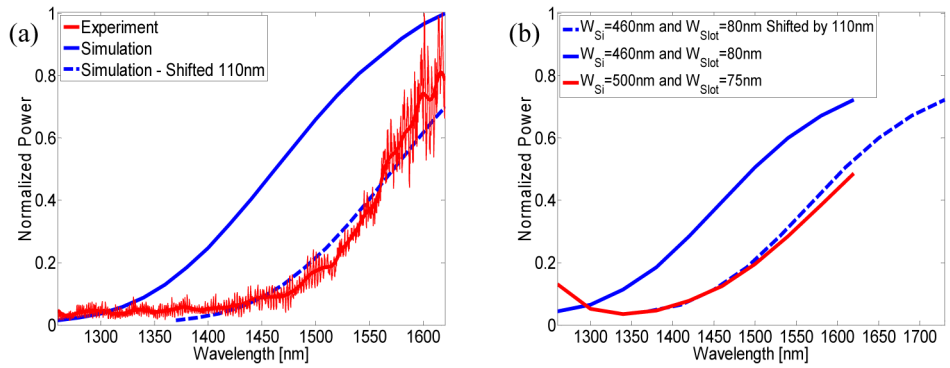

Fig. 3. (a) Comparison of the experimental and simulation results of the plasmonic air-slot coupler. (b) Comparison of the simulation results of two plasmonic air-slot couplers of different widths.

In order to investigate the propagation loss of the plasmonic waveguide, we fabricated two plasmonic air-slot waveguides of different lengths (L_p = 500 nm and 2000 nm). The experimental results (see Fig. 4) show that the longer plasmonic waveguide resulted in a

#254165 Received 23 Nov 2015; revised 16 Feb 2016; accepted 19 Feb 2016; published 7 Apr 2016

reduction in the transmitted power into the output silicon waveguide by about 3 dB compared with the measured power of the shorter plasmonic waveguide. This measurement cannot be used to calculate the propagation loss of the plasmonic waveguide because the two plasmonic devices are not identical due to the limitations in the fabrication tools. High precision fabrication techniques are needed to get the same width and length of the air-slot coupler inside both devices that have different lengths.

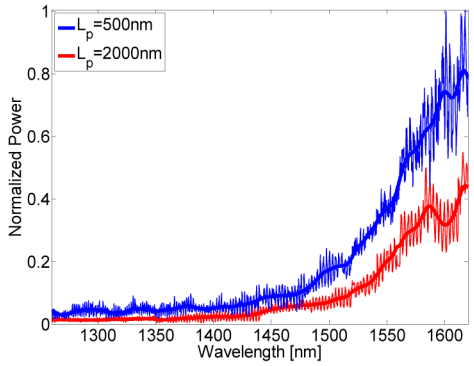

Fig. 4. Experimental results of two plasmonic air-slot couplers: one had a length of 500 nm and the other one had a length of 2000 nm.

4. Analysis of the sensitivity of the design to different fabrication challenges

In order to show the sensitivity of our proposed plasmonic air-slot coupler to different fabrication challenges, we investigated through numerical simulations the effect of changing various parameters of the design on the spectrum response of our device. The parameters that we changed were [see Fig. 5(a)]: the length of the air-slot waveguide inside the silicon waveguide L_c, the width of the silicon waveguide W_{Si}, the width of the plasmonic slot waveguide W_{Slot}, and the misalignment between the position of the plasmonic slot waveguide with respect to the center of the silicon waveguide S. The optimum values that we used for L_c, W_{Si}, W_{Slot}, S, and L_p were 50 nm, 460 nm, 80 nm, 0 nm, and 500 nm, respectively. We studied the effect of changing one parameter on the spectrum response while keeping the remaining parameters at their optimum values. We found that changing L_c from 0 nm to 400 nm resulted in a change in the spectrum response shape mainly due to the Fabry-Perot cavity-like effect in addition to the impedance mismatch between the silicon and slot waveguides which is a function of wavelength [see Fig. 5(b)]. The maximum coupling efficiency occurred when L_c = 50 nm. We also found that the cut-off wavelength can be controlled by changing W_{Si} [see Fig. 5(c)] or W_{Slot} [see Fig. 5(d)]. Changing W_{Si} from 420 nm to 500 nm resulted in shifting the cut-off wavelength from about 1150 nm to 1400 nm (i.e., right shift). Whereas, changing W_{Slot} from 40 nm to 120 nm resulted in shifting the cut-off wavelength from about 1400 nm to 1250 nm (i.e., left shift). This shift occurs because as the waveguide's width changes, the mode size changes and consequently, the impedance mismatch between the silicon and slot waveguide changes. In Fig. 3(a), the experimental curve was shifted by 110 nm because the width of the silicon waveguide was increased by about 40 nm (i.e., W_{Si} = 500 nm). Finally, we found that changing S from 0 nm to 80 nm resulted in a reduction in the coupled power into the plasmonic slot waveguide due to the reduction in the overlapped area between the mode supported by the slot waveguide and that of the silicon waveguide [see Fig. 5(e)]. For example, at a wavelength of 1800 nm, the coupled power dropped by a factor of 10 (i.e., 70% to 7%), when the slot waveguide was shifted by 80 nm. From these simulation results, it is obvious that the spectrum response of the plasmonic coupler is strongly dependent on L_c, W_{Si}, W_{Slot}, and S which are affected by the lithography and etching bias.

#254165 Received 23 Nov 2015; revised 16 Feb 2016; accepted 19 Feb 2016; published 7 Apr 2016

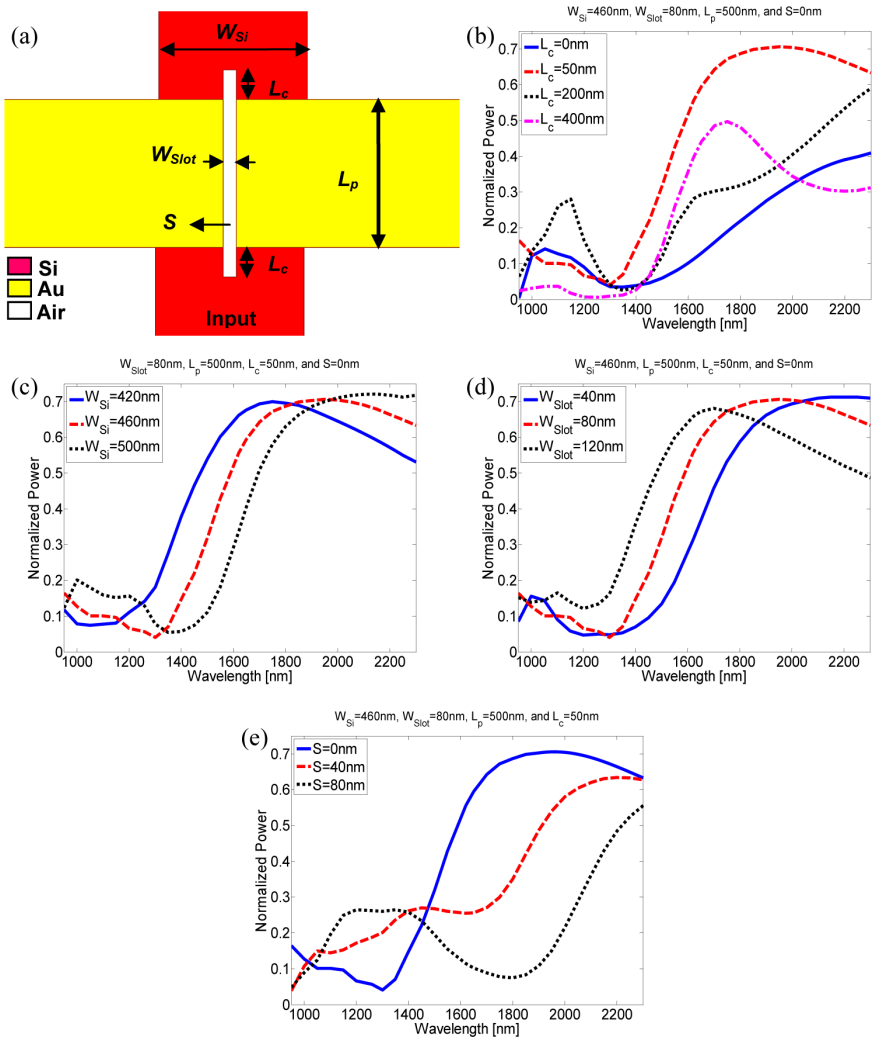

Fig. 5. (a) Schematic of the air-slot coupler. (b-e) Dependence of the spectrum response of the coupler on the length of the air-slot waveguide inside silicon L_c, the width of the silicon waveguide W_{Si}, the width of the plasmonic slot waveguide W_{Slot}, and the misalignment between the position of air-slot waveguide with respect to the center of the silicon waveguide S, respectively.

5. Conclusions

We experimentally showed that an air-slot coupler can be used to couple light from a silicon waveguide into an MIM plasmonic waveguide. Our experimental results are in good agreement with the theoretical calculation results. The experimental results can be improved if high precision fabrication techniques are used. We showed the dependence of the coupling efficiency on the width of the silicon waveguide in addition to the length, width, and position of the air-slot waveguide. We found that the cut-off wavelength can be shifted to higher or lower wavelengths which eventually affects the coupling efficiency. We also found that high coupling efficiency occurs only when the air-slot waveguide is fabricated at the center of the silicon waveguide. The high coupling efficiency happens because the mode size in the air-slot waveguide matches that inside the silicon waveguide.

#254165 Received 23 Nov 2015; revised 16 Feb 2016; accepted 19 Feb 2016; published 7 Apr 2016